Classification: Biological Sciences (Environmental Sciences)

Reduced Impact Logging Minimally Alters Tropical Rainforest Carbon and Energy Exchange

Scott D. Miller[1], Michael L. Goulden[2], Lucy R. Hutyra[3], Michael Keller[4], Scott R. Saleska[5], Steven C. Wofsy[6], Adelaine Michela Silva Figueira[7], Humberto R. da Rocha[8], Plinio B. de Camargo[9]

1. Atmospheric Sciences Research Center, State University of New York at Albany, 251 Fuller Road, Albany, NY 12203
2. Department of Earth System Science, University of California, Croul Hall, Irvine, CA 92697.
3. Department of Geography and Environment, Boston University, Stone Science 439, Boston, MA, 02215
4. International Institute of Tropical Forestry, USDA Forest Service, San Juan, Puerto Rico 00928
5. Department of Ecology and Evolutionary Biology, University of Arizona, Tuscon, Arizona, 85721
6. Department of Earth and Planetary Sciences, Harvard University, Cambridge, 29 Oxford St., Cambridge, MA 02138
7. Department of Biology, Federal University of Western Pará, Av Marechal Rondon Santarem, Pará, Brazil, 68040-070
8. Department of Atmospheric Sciences, University of Sao Paulo, Rua do Matão 1226, Sao Paulo, Brazil, 05508-090.
9. CENA, University of Sao Paulo, Av Centenário 303, Piracicaba, Sao Paulo, Brazil, 13416-000.

* Corresponding author:
Scott D. Miller
Atmospheric Sciences Research Center
State University of New York at Albany
Albany, NY 12203
Phone 518 437-8799
Fax 518 437-8758
smiller@albany.edu

Abstract

We used eddy covariance and ecological measurements to investigate the effects of Reduced Impact Logging (RIL) on an old-growth Amazonian forest. Logging caused small decreases in gross primary production, leaf production, and latent heat flux, which were roughly proportional to canopy loss, and increases in heterotrophic respiration, tree mortality, and wood production. The net effect of RIL was transient, and treatment effects were barely discernable after only one year. RIL appears to provide an economically viable strategy for managing tropical forest that minimizes the potential risks to climate associated with large changes in carbon and water exchange.

\body

Introduction

Deforestation in the tropics affects the land-atmosphere exchange of trace gases and energy in ways that may impact regional and global climate. Tropical deforestation contributed 16% (1.5 Pg C yr^{-1}) of human-induced CO_2 emissions during 2000-2006 (1), while increasing land-surface albedo and decreasing available energy and evapotranspiration (2). The changes in surface energy exchange and increase in atmospheric CO_2 associated with large-scale tropical deforestation are predicted to alter precipitation patterns (3, 4) and cause a net warming of global climate (5, 6). The avoidance of tropical deforestation as a means to slow the rise of atmospheric carbon dioxide, while maintaining the role of forest in the water and energy cycles and sustaining biodiversity and other environmental services, is a key climate change mitigation goal (e.g., the United Nations program Reducing Emissions from Deforestation and Forest Degradation – UN-REDD) (7, 8).

The harvesting of marketable trees by selective logging in the Brazilian Amazon has occurred at an areal rate comparable to deforestation ($1\text{-}2 \times 10^4$ $km^2 yr^{-1}$ between 1996-2002) (9-11). Conventional logging (CL) is highly damaging to forest canopy, residual vegetation, and soil (12); estimates of CO_2 emissions due to Amazonian CL are as high as 25% of the deforestation source (9). Reduced Impact Logging (RIL) is intended to minimize the disruption of tropical forest carbon and water cycles (13) via pre-harvest tree selection and vine cutting, directional felling, and planned extraction (skid) trails and log decks. RIL has been shown to provide economic returns comparable to conventional logging (14) while maintaining future harvest yields (15) and reducing canopy destruction (12, 16, 17). However, the effects of RIL on land-atmosphere gas and energy exchange have not been well quantified.

We report measurements of forest carbon, water and energy exchange in the Brazilian Amazon to characterize and quantify the response of tropical forest to RIL, as part of the Large-Scale Biosphere-Atmosphere Experiment in Amazonia (18). Two sites in the Tapajos National Forest were studied, denoted by distance south of Santarem, Para (Fig. S1, Supplemental Information): "km 67" (un-logged control site, 2.85667 S, 54.958889 W) and "km 83" (logged site, 3.01803 S, 54.97144 W). The logging was conducted by a local commercial firm (Empresa Agropecuária Treviso Ltda), with oversight from the Brazilian Institute for the Environment and Renewable Resources (IBAMA). Parallel measurements at control and logged sites began 6-12 months prior to logging, and continued at least 29 months afterward. Our measurements focused on aspects of land-atmosphere exchange that are expected to affect climate: changes to carbon and energy fluxes, net carbon storage, soil moisture, and albedo.

Results

Loggers cut 3.6 trees ha^{-1}, which contained 12.5-17 Mg C ha^{-1} and accounted for 7-10% of the forest's initial above ground live biomass (AGLB, 168 Mg C ha^{-1}, Table S1, Supplemental Information). The rate of wood extraction (5.0 -6.8 Mg C ha^{-1}) was slightly less than the average log removal for the overall Amazon basin (7.3 Mg C ha^{-1} of bole wood removed (11)). Fifteen additional trees were killed or damaged for each tree logged at km 83 (19), and logging added 12.5-17.2 Mg C ha^{-1} of coarse woody debris (CWD) to the forest floor, including 2.7-3.6 Mg C ha^{-1} of bole wood, 5.0-6.9 Mg C ha^{-1} of logged tree crowns, and 4.8-6.7 Mg C ha^{-1} of damaged biomass from adjacent trees. Standing dead trees accounted for another 0.7-1.0 Mg C ha^{-1}, and the total carbon either removed or killed was 18.2-25.0 Mg C ha^{-1}, or 11-15% of initial AGLB. Logging created 2.5 canopy gaps ha^{-1}, decreasing the coverage of intact canopy from 96% to 88% (20). The extent of canopy destruction was far less than the 30% loss reported for CL (12).

Logging had a marked effect on the patterns of production. We partitioned aboveground wood production into three size classes: small subcanopy trees with diameter at breast height (1.3 m, DBH) 10-35 cm, medium mid-canopy trees with DBH 35-55 cm, and large upper-canopy trees with DBH 55-100 cm (21). Wood production before logging exhibited a strong maximum corresponding to tree heights at the mid-to-upper canopy levels (~25 m, Fig. 1a open squares). Wood production in the lower canopy more than doubled following logging (Fig. 1a, solid circles and hatched area), and the mean tree height of production descended from 26 m to 24 m. Stimulation of tree growth, especially near gaps, was likely caused by increased light penetration and facilitated by the low levels of damage to the canopy and subcanopy (22).

The changing patterns of production among tree size classes (Fig. 1a) did not translate into large shifts in whole-stand carbon fluxes, as measured by eddy covariance. The time series of gross photosynthesis (GEE, positive flux indicates uptake by the forest, Fig. 2a) and respiration (R, positive flux indicates loss from the forest, Fig. 2b) showed no distinct changes following logging (Fig. 2a,b). Differences in GEE and R between logged and control sites were smaller than the uncertainty in the monthly-averaged time series (overlapping shaded regions in Fig. 2a,b). The small effect of RIL on the carbon fluxes is emphasized by the similarity of NEE (R-GEE), both magnitude and seasonal variation, between logged and control sites (Fig. 2c).

Likewise, the cumulative rates of net and gross CO_2 exchange did not change markedly following logging. We summed the fluxes for 6 and 12-month periods, and calculated the differences between sites (Δ=the difference between km 83 and km 67) to obtain ΔGPP, ΔR, and ΔNEE before and after logging (Table S2, Supplemental Information). GPP at km 83 decreased relative to km 67 ($\Delta GPP_{postlog} - \Delta GPP_{prelog}$ was negative) by 2-3 Mg C $ha^{-1}yr^{-1}$ following logging (Fig. 3a,b), which corresponds to a ~10% decline that is comparable to the observed decrease in the area of intact forest canopy. R at km 83 increased slightly in the first year following logging ($\Delta R_{postlog} - \Delta R_{prelog}$ was positive), and subsequently declined in years 2 and 3. $\Delta NEE_{postlog} - \Delta NEE_{prelog}$ was 2-3 Mg C $ha^{-1}yr^{-1}$ during the first year after logging (Fig. 3c), corresponding to a net release of carbon to the atmosphere. ΔNEE was indistinguishable from the pre-logging period in years 2 and 3 (Fig 3c).

Ecosystem carbon budgets were constructed before and after logging (Fig. 4a,b and Table S4, Supplemental Information). Total respiration was partitioned into autotrophic (R_a) and heterotrophic (R_h) sources by combining the micrometeorological and ecological measurements (see Materials and Methods). Autotrophic respiration decreased by 9% (3 Mg C $ha^{-1}yr^{-1}$), which was similar to the declines in GPP, intact canopy area, and AGLB. About half the R_a decrease was offset by increasing decomposition (R_h), resulting in a 1.5 Mg C $ha^{-1}yr^{-1}$ decrease in total R (Fig. 3b). Similarly, much of the increase in wood production at the logged site was offset by a 10% decrease in leaf production (NPP_{leaf}), resulting in a small increase in total NPP (assuming constant NPP_{root}). Interestingly, the NPP:GPP ratio, a measure of carbon use efficiency, increased from 0.29 to 0.35.

The logging had a marked effect on the local patterns of soil water content and withdrawal. Soil water extraction following logging was calculated from the observed changes in soil moisture during the dry season (Aug-Oct) in two 10-m profiles at km 83, one in intact forest and the other in a logging gap (23). The water withdrawal from the soil averaged 8.4 mm d^{-1} in the intact forest and 5.9 mm d^{-1} in the logging gap over the 90-day period. A larger proportion of water was extracted from shallower depths in the logging gap, and the mean depth of withdrawal shifted from 4 m in the intact forest to 3 m in the logging gap (Fig. 1b, hatched area versus shaded area). The 40% decrease in water withdrawal in the gap was attributed to the loss of canopy and hypothesized decrease in live root density. The mature trees that were harvested may have been deeply rooted compared to the small stems that grew up in the gap.

Logging had modest and transient effects on the water and energy fluxes by the entire ecosystem. Changes in water and heat flux were smaller than the inter-seasonal and inter-annual variability (Fig. 2d,e, and Table S2, Supplemental Information). Sensible heat flux at the logged site increased by several Wm^{-2} relative to the control site, corresponding to a change of about 10% (Fig. 3d). Latent heat flux decreased by a slightly larger amount (3-4 Wm^{-2}) (Fig. 3e). The ratio of sensible to latent heat flux (the Bowen ratio) increased from 0.2 to 0.3 at the logged site in the first year after logging, but returned to the pre-logging ratio by year 3. Logging had no discernable effect on the km 83 albedo determined by NASA's MODIS sensors (Table S3, Supplemental Information). The proportional changes in the heat fluxes and canopy loss, and the lack of change in albedo, imply the shifts in sensible and latent heat flux were driven by the loss of canopy and not a change in available energy.

Discussion

RIL for the 3130 ha tract logged at Tapajos National Forest was highly profitable (24). Overall revenue from wood was 830 \$US ha^{-1}, compared with costs of 610 \$US ha^{-1}; thus, RIL resulted in an internal rate of return (IRR) of 36%, much higher than the most profitable cattle projects studied in the Amazon (IRR up to 12%) (24). The km 83 logging generated high-paying jobs by local standards at a rate of one person employed for every 14 ha logged, with 60% of positions filled by residents of local communities by the end of the project.

Logging resulted in a small, transient net source of CO_2 to the atmosphere, mostly in the first year, presumably due to the rapid decomposition of fine logging debris (25, 26). The first-year carbon emission at the logged site was 2.4-2.7 Mg C ha^{-1}, which is less than 10% of GPP and less than 2% of the original aboveground biomass. RIL-induced greenhouse gas forcing due to soil emissions of N_2O, CH_4, and CO_2 were small (27). Off-site carbon emissions due to decomposition or combustion of short-lived products and mill waste were estimated to be 3 Mg C ha^{-1}, assuming one-third of the bole wood removed from the site ended up as long-lived products. The total equivalent carbon emission was ~6 Mg C ha^{-1}, less than 4% of the forest's 168 Mg C ha^{-1} AGLB.

Changes to the forest-atmosphere fluxes were near our detection limits, underscoring the relatively small effect of RIL (Fig. 4, Tables S3 and S4, Supplemental Information). The small shifts in ΔNEE and Bowen ratio lasted only 1 to 3 years, and the forest lost only a small fraction of its biomass carbon to the atmosphere. Figures 2 and S2 suggest carbon uptake at the logged site accelerated relative to the control site throughout the post-logging period. The ability of the forest to maintain NPP despite the loss of canopy, and the increased allocation of carbon to stem production, point to a rapid restoration of biomass following disturbance. The changes in several key ecosystem processes (GPP, NPP_{leaf}, H_L) in direct proportion to canopy loss underscore the importance of minimizing canopy destruction.

The ~6 Mg C ha^{-1} total equivalent carbon emission due to RIL was much smaller than the 150 Mg C ha^{-1} (90% of AGLB) that would have been released by deforestation (28). The albedo was unaffected by RIL, whereas local deforestation increased albedo by 0.01 to 0.03 (Table S3, Supplemental Information), and tower-based measurements in the southwestern Amazon showed a 60% albedo increase following deforestation (2). The initial shifts in energy exchange and Bowen Ratio with RIL did not differ dramatically from the 20-40% changes in sensible and latent heat flux and doubling of Bowen Ratio reported with conversion to pasture in the southwestern Amazon (2). But the changes in energy exchange following RIL were brief and persisted for just one or two years, whereas changes associated with deforestation are sustained.

Our measurements captured only the immediate effects of RIL on carbon and energy fluxes; the effects on tree mortality, demographic shifts, and changes in wood production beyond the 3-year study interval are uncertain. The effects of logging on floristic composition and biodiversity were also not considered, and it is uncertain how the forest would respond to more intense or repeated logging. Nonetheless, with net carbon emission just 4% of that typical of deforestation, RIL has the potential to significantly reduce the impact of tropical land use on land-atmosphere exchange. About half of the net CO_2 emission was estimated to occur from the harvested boles, suggesting that improvements in mill processing and conversion of biomass to energy could contribute further to climate change mitigation.

Cumulative deforestation in the Brazilian Amazon reached 18% of the original forested area in 2008 (10). At an average rate of 1.7×10^4 km^{2}y^{-1} (2001-2008) (10), business-as-usual scenarios imply that as much as 35% of Amazon rain forests could be cleared by 2040, contributing up to 4% of anthropogenic carbon emissions, altering the energy balance, and warming the climate. In contrast, our study demonstrates that RIL had small effects on the major drivers of climate warming associated with tropical deforestation. RIL appears to provide an economically viable strategy for managing tropical forest that minimizes the potential risks to climate associated with large changes in carbon and water exchange.

Materials and Methods

The logged site was within a 700-ha area that was part of a larger, 3130-ha Reduced Impact Logging (RIL) demonstration project over a 5-year period beginning in 1999. The logging at the km 83 flux tower site occurred between Aug and Dec 2001, resulting in a logged area that extended 1-to-3 km east and north of the flux tower.

Canopy Gaps

After the logging, gap location, size, and shape were mapped in a 600 m by 300 m area that extended 500 m to the northeast of the logged-site flux tower. The logging created 44 new gaps, which ranged in size from single tree falls, which were ~10 m across, to log landings used to temporarily store boles, which were ~50 m across (20).

Ecological measurements

Initial surveys of tree DBH were used along with allometric equations developed for moist tropical forests (29) to calculate above ground live biomass in 1999, 2001, and 2005 at the control site (30) and 2000 at the logged site (31). Large (55-100 cm) and medium (35-55 cm) trees were measured in a 20-ha plot at the control site, and a 48-ha area at the logged site, while small (10-35 cm) trees were measured in a 4-ha sub-sample at the control site, and a 1.8-ha sub-sample at the logged site. The survey data sets are available online (32, 33).

Wood production was measured using dendrometer bands to monitor changes in tree DBH (34). At the control site, 763 bands were installed on 529 small, 119 medium, and 115 large trees in a 20-ha area east of the flux tower in 1999 (30). At the logged site, 691 bands were installed on 363 small, 223 medium, and 105 large trees in an 18-ha area east of the tower between Nov 2000-Feb 2001. DBH increments were measured each 4 weeks at the control site and each 6 weeks at the logged site. The cumulative DBH increment for each tree at the control site was calibrated so that the long-term increment matched the measured change in DBH between the 2001 and 2005 surveys. Tree mass and height were calculated for each DBH measurement (35, 21), and wood production between measurement intervals was calculated from changes in tree mass. For each tree size class, wood production was calculated as the product of the mean per tree growth rate and the stem density for that size class (Table S5, Supplemental Information). Uncertainties in wood production rates reflect the variability (95% confidence interval) in growth rates within a tree size class. The wood production data sets are available online (36, 37).

Litterfall (NPP_{leaf}), including leaves, fruit, and wood were collected in litter baskets east of each of the flux towers at 2-week intervals, and were used to calculate fine litter production. The litterfall data are available online (38, 36).

Micrometeorological measurements

Carbon and energy flux at each site were measured from a 67-m-tall, 46-cm-triangular-cross-section tower (Rohn 55G, Peoria IL). The logged site tower operated for 1353 days (32,496 hours) between Jul 1, 2000 and Mar 13, 2004 (39). The control site tower operated for 1733 days (41,592 hours) between Apr 13, 2001 and Jan 9, 2006 (40). Measurements at both sites were terminated by tree falls that destroyed the towers. The CO_2 profile between the surface and the height of the eddy covariance instrumentation was measured and used to calculate changes in CO_2 storage within the air column below the flux sensors (F_s). Turbulent CO_2 flux (F_c) and storage were combined to estimate Net Ecosystem Exchange (NEE) for each flux interval as $NEE = F_c + F_s$. Data retention rates for carbon and water fluxes were 75-88% at both sites. Methodology used to measure and calculate fluxes, fill data gaps, and to correct for flux loss during conditions with poor vertical mixing (u_*-filter) have been published (40, 31, 41), and the flux data sets are available online (42-44).

Missing meteorological variables and turbulent fluxes were gap-filled using mean diurnal variation with a 40-day window (41). Missing NEE was filled using a light-response model (45). Uncertainties in NEE due to sampling uncertainty and gap filling of missing data were estimated using a bootstrap method (41). The uncertainty in the carbon fluxes (NEE, GPP, R) due to the u_*-filter was estimated by calculating the carbon fluxes using a range of u_*-filter cutoffs from 0.17 m s^{-1} to 0.27 m s^{-1} to generate time series of NEE, GPP, and R representing lower and upper bounds of plausible carbon exchange (e.g., $NEE_{0.17}$ and $NEE_{0.27}$). The uncertainty in the carbon exchange due to the choice of the u_*-filter cutoff was calculated as the larger of the differences $NEE_{0.22}$-$NEE_{0.17}$ (lower bounds) and $NEE_{0.27}$-$NEE_{0.22}$ (upper bounds), and was added to the sampling and gap filling uncertainty estimates to calculate the total uncertainty at each site (Fig. 2a-c, and Table S2, Supplemental Information, top section). However, it was previously shown that a u_*-filter cutoff of 0.22 m s^{-1} (e.g., $NEE_{0.22}$) provided the best estimate of ecosystem respiration at both sites (41); therefore, the u_*-filtering uncertainty was not included in the *differences* in carbon fluxes between the sites (ΔGPP, ΔR, ΔNEE) in Figures 3a-c, and Table S2, Supplemental Information, bottom section).

Soil moisture measurements

Soil moisture measurements were made at the logged site from Mar 2002 to Dec 2003 in two 10-m deep soil pits (1x2 m^2 area) within 50 m of the micrometeorological tower (23). Both pits were within the selectively logged area: one within an intact area of forest, the other within a gap created by the logging. Soil water content was measured at 0.5 Hz using water content reflectometers (CS615-G, Campbell Scientific, Logan, Utah, USA) installed horizontally into the walls of the pits at 0.15, 0.3, 0.6, 1, 2, 3, 4, 6, 8, and 10 m. Soil water withdrawal was calculated as the difference between the profile measured at the beginning (first 2 weeks of Aug 2002) and end (last two weeks of Oct 2002) of the dry season. The soil moisture data sets are available online (46).

Albedo

Satellite 8-day composite time series of 500m-MODIS albedo for the km 83 and km 67 sites, and also for a nearby pasture (km 77), were obtained from the Distributed Active Archive Centers (DAACs) Land Products website (http://daac.ornl.gov/MODIS/). The data included 1 year before logging and 3 years after logging at each site (Table S3, Supplemental Information). Shortwave albedo data was used with default solar zenith angle (local solar noon) and optical depth (0.2). At the forest sites, mean albedo for each 8-day composite was calculated for an 18.8 ha area east of the flux tower, 3.5 km (7 pixels) in east-west direction and 2.5 km (5 pixels) in the north-south direction. At the pasture site, a 0.5 km^2 area (2 pixels east-west, 1 pixel north-south) was used. The uncertainty in albedo was estimated by bootstrapping.

Ecosystem carbon budget

An ecosystem carbon budget at the logged site was constructed for the year before logging and the 3-year period after logging by combining the micrometeorological and ecological measurements. The relationships between the carbon pools and fluxes are sketched in Figure 4 and tabulated in Table S4 (Supplemental Information).

For micrometeorological fluxes (GPP, R, NEE), the pre-logging flux ($X_{prelog,\ 12\ mos.}$) was calculated as the average for the 12-month period prior to logging. The difference between the post- and pre-logging flux at the logged site, δX_{total}, was assumed to include contributions due to the logging, $\delta X_{logging}$, and due to inter-annual differences in climate or "weather", $\delta X_{weather}$, such that $\delta X_{total} = X_{postlog} - X_{prelog} = \delta X_{logging} + \delta X_{weather}$, where, for simplicity, measurement error is not denoted; however, its calculation is detailed below. The weather-induced contribution was assumed to be equal at the two sites, $\delta X_{weather} = \delta X_{weather,\ km\ 67}$, and the difference in post- and pre-logging flux at km 67 (the unlogged site) was assumed entirely due to weather, $\delta X_{total,\ km67} = \delta X_{weather,\ km67} = X_{postlog,\ km67} - X_{prelog,\ km67}$. Rearranging these expressions gives $\delta X_{logging} = \left(X_{postlog} - X_{postlog,\ km67}\right) - \left(X_{prelog} - X_{prelog,\ km67}\right) = \Delta X_{postlog} - \Delta X_{prelog}$, where the Δ notation was used in the main text and plotted in Figure 3. This expression was evaluated using only periods with *in situ* data at the both sites. The post-logging flux was calculated as the sum $X_{postlog} = X_{prelog,\ 12mo} + \delta X_{logging}$. The uncertainty in the ΔX terms was calculated as the square root of sum of the squared uncertainties of X at the logged and unlogged sites (i.e., their errors were assumed uncorrelated). Similarly, the uncertainty in δX was calculated as the square root of sum of the squared uncertainties of ΔX_{prelog} and $\Delta X_{postlog}$ (i.e., errors before and after logging were assumed uncorrelated).

Net Primary Production (NPP) was calculated as the sum of wood, leaf, and root production, $NPP = NPP_{wood} + NPP_{leaf} + NPP_{root}$, where wood production and leaf production at each site were measured by dendrometers and litter baskets (see Materials and Methods and Table S3), and NPP_{root} was assumed constant and equal to 2.5 ± 0.5 Mg C ha^{-1}yr^{-1} (22), where 20% uncertainty in root production was assumed (47) . Litter production (above and below ground) was calculated as sum of NPP_{leaf} and NPP_{root}, assuming belowground root litter was in steady state with root production. The uncertainty in NPP and in litter production was calculated as the square root of the sum of squared uncertainties of the component fluxes (i.e., uncertainties were assumed uncorrelated).

Mortality at the logged site before logging (1.7 Mg C ha^{-1} yr^{-1}) was assumed in steady state with wood production (31), and after logging was 4.5 Mg C ha^{-1} yr^{-1} (22). Mortality at the control site was 2.4 Mg C ha^{-1} yr^{-1} (30). The uncertainty in mortality at the logged site was assumed to be 30% (30). The change in live biomass was calculated as NPP minus the sum of mortality and litter production, and the change in necromass calculated as NEP minus the change in live biomass (Fig. 4). The uncertainties in changes in live and dead biomass were calculated as the square root of the sum of squares of the component fluxes.

Autotrophic respiration (Ra) was calculated as GPP-NPP, and decomposition (heterotrophic respiration, Rh) was calculated as Rh=R-Ra (Fig. 4). The uncertainties in Rh and Ra were calculated as the square root of the sum of squares of the component fluxes.

Additional uncertainty was included in the carbon budget (Table S4, Supplemental Information) to account for the fact that overlapping data at the control and logged sites prior to logging covers only part of a year (seasonality effect). The carbon budget was re-calculated using only data collected between Mar-Sep in each year after logging, to match with the months of data overlap in the pre-logging period. For each carbon flux in the budget, the magnitude of the difference between the budget calculated using all months and using only Mar-Sep was used as an estimate of this additional uncertainty, and was added to the statistical sources of uncertainty described above.

Acknowledgements

This work was supported by the U.S. National Aeronautics and Space Administration awards to the University of California at Irvine (Goddard NCC5-280), Harvard University (NNG06GG69A), and the State University of New York at Albany (NNG06GD29A). We thank Mary Menton, Antonio Oviedo, Helber Freitas, Marcy Litvak, Edward Lloyd Read, Robert

Elliot, Chris Doughty, Dan Hodkinson, Lisa Zweede, Bethany Reed, and Johan Zweede for logistical and field support; IBAMA, NASA and INPE for agency support; and CNPq for student stipends. We are grateful to the Brazilian Ministry of Science and Technology (MCT) for their leadership of the Large-Scale Biosphere–Atmosphere Experiment in Amazonia (LBA) and to Brazil's National Institute for Amazon Research (INPA) for their management of that program.

References

1. Canadell JG et al. (2007) Contributions to accelerating atmospheric CO2 growth from economic activity, carbon intensity, and efficiency of natural sinks. *Proceedings of the National Academy of Sciences of the United States of America* 104:18866-18870.

2. Von Randow C et al. (2004) Comparative measurements and seasonal variations in energy and carbon exchange over forest and pasture in South West Amazonia. *Theoretical and Applied Climatology* 78:5–26.

3. Dickinson RE et al. (1989) Implications of Tropical Deforestation for Climate: A Comparison of Model and Observational Descriptions of Surface Energy and Hydrological Balance [and Discussion]. *Philosophical Transactions of the Royal Society of London. Series B, Biological Sciences* 324:423–431.

4. Werth D, Avissar R (2002) The local and global effects of Amazon deforestation. *J. Geophys. Res* 107.

5. Salati E, Nobre CA (1991) Possible climatic impacts of tropical deforestation. *Climatic change* 19:177–196.

6. Bala G et al. (2007) Combined climate and carbon-cycle effects of large-scale deforestation. *Proceedings of the National Academy of Sciences* 104:6550.

7. Sist P, Ferreira FN (2007) Sustainability of reduced-impact logging in the Eastern Amazon. *Forest Ecology and Management* 243:199-209.

8. Miles L, Kapos V (2008) Reducing greenhouse gas emissions from deforestation and forest degradation: global land-use implications. *Science* 320:1454.

9. Asner GP et al. (2005) Selective Logging in the Brazilian Amazon. *Science* 310:480-482.

10. INPE (2010) Monitoring of the Brazilian Amazon forest by satellite: 1988-2009. Available at: www.inpe.br.

11. Nepstad DC et al. (1999) Large-scale impoverishment of Amazonian forests by logging and fire. *Nature* 398:505-508.

12. Pereira R, Zweede J, Asner GP, Keller M (2002) Forest canopy damage and recovery in reduced-impact and conventional selective logging in eastern Para, Brazil. *Forest Ecology and Management* 168:77-89.

13. Uhl C et al. (1997) Natural resource management in the Brazilian Amazon. *Bioscience* 47:160–168.

14. Holmes TP et al. (2002) Financial and ecological indicators of reduced impact logging performance in the eastern Amazon. *Forest Ecology and Management* 163:93-110.

15. Keller M, Asner GP, Silva J, Palace M (2004) in *Working Forests in the Neotropics: Conservation through Sustainable Management?*, eds Zarin D, Alavalapati J, Putz FE, Schmink M (Columbia University Press, New York), pp 41-63.

16. Pinard MA, Putz FE (1996) Retaining forest biomass by reducing logging damage. *Biotropica* 28:278-295.

17. Veríssimo A, Barreto P, Mattos M, Tarifa R, Uhl C (1992) Logging impacts and prospects for sustainable forest management in an old Amazonian frontier: the case of Paragominas. *Forest ecology and management* 55:169–199.

18. Keller M et al. (2004) Ecological research in the Large-scale Biosphere-Atmosphere Experiment in Amazonia: Early results. *Ecological Applications* 14:S3-S16.

19. Sousa A et al. (2008) LBA-ECO CD-04 Post-logging Damage Survey, Logged Forest Site, km 83 Tower Site, Tapajos National Forest. *Oak Ridge National Laboratory Distributed Active Archive Center*. Available at: http://daac.ornl.gov.

20. Miller SD, Goulden ML, da Rocha HR (2007) The effect of canopy gaps on subcanopy ventilation and scalar fluxes in a tropical forest. *Agricultural and Forest Meteorology* 142:25-34.

21. Nogueira EM, Nelson BW, Fearnside PM, França MB, Oliveira Á (2008) Tree height in Brazil's ‘arc of deforestation’: Shorter trees in south and southwest Amazonia imply lower biomass. *Forest Ecology and Management*.

22. Figueira AM et al. (2008) Effects of selective logging on tropical forest tree growth. *JGR-Biogeosciences*..

23. Bruno RD, da Rocha HR, de Freitas HC, Goulden ML, Miller SD (2006) Soil moisture dynamics in an eastern Amazonian tropical forest. *Hydrological Processes* 20:2477-2489.

24. Bacha CJ, Rodriguez LC (2007) Profitability and social impacts of reduced impact logging in the Tapajos National Forest, Brazil–A case study. *Ecological Economics* 63:70–77.

25. Bormann FH, Likens GE (1979) Pattern and process in a forested ecosystem.

26. Sprugel DG (1985) Natural disturbance and ecosystem energetics.

27. Keller M et al. (2005) Soil–atmosphere exchange of nitrous oxide, nitric oxide, methane, and carbon dioxide in logged and undisturbed forest in the Tapajós National Forest, Brazil. *Earth Interactions* 9:1–28.

28. Houghton RA et al. (2000) Annual fluxes of carbon from deforestation and regrowth in the Brazilian Amazon. *Nature* 403:301.

29. Keller M, Palace M, Hurtt G (2001) Biomass estimation in the Tapajos National Forest, Brazil Examination of sampling and allometric uncertainties. *Forest Ecology and Management* 154:371–382.

30. Rice AH et al. (2004) Carbon balance and vegetation dynamics in an old-growth Amazonian forest. *Ecological Applications* 14:55–71.

31. Miller SD, Goulden ML, Menton MC, da Rocha HR, de Freitas HC (2004) Biometric and micrometeorological measurements of tropical forest carbon balance. *Ecological Applications* 14.

32. Wofsy SC, Saleska SR, Pyle EH, Hutyra LR (2008) LBA-ECO CD-10 Tree DBH Measurements at the km 67 Tower Site, Tapajos National Forest. *Oak Ridge National Laboratory Distributed Active Archive Center*. Available at: http://www.daac.ornl.gov.

33. Menton M et al. (2008) LBA-ECO CD-04 Biomass Survey, Logged Forest Site, km 83 Tower Site, Tapajos National Forest. *Oak Ridge National Laboratory Distributed Active Archive Center*. Available at: http://daac.ornl.gov.

34. Liming FG (1957) Homemade dendrometers. *Journal of forestry* 55:575–577.

35. Chambers JQ, Santos J, Ribeiro RJ, Higuchi N (2001) Tree damage, allometric relationships,

and above-ground net primary production in central Amazon forest. *Forest Ecology and Management* 152:73–84.

36. Rice AH et al. (2008) LBA-ECO CD-10 Ground-based Biometry Data at km 67 Tower Site, Tapajos National Forest. *Oak Ridge National Laboratory Distributed Active Archive Center*. Available at: http://www.daac.ornl.gov.

37. Sousa A et al. (2008) LBA-ECO CD-04 Dendrometry, Logged Forest Site, km 83 Tower Site, Tapajos National Forest. *Oak Ridge National Laboratory Distributed Active Archive Center*. Available at: http://daac.ornl.gov.

38. Figueira AM et al. (2008) LBA-ECO CD-04 Leaf Litter Data, Logged Forest Site, km 83 Tower Site, Tapajos National Forest. *Oak Ridge National Laboratory Distributed Active Archive Center*. Available at: http://daac.ornl.gov.

39. Goulden ML et al. (2004) Diel and seasonal patterns of tropical forest CO2 exchange. *Ecological Applications* 14:42-54.

40. Hutyra LR et al. (2007) Seasonal controls on the exchange of carbon and water in an Amazonian rain forest. *J. Geophys. Res* 112.

41. Saleska SR et al. (2003) Carbon in Amazon Forests: Unexpected Seasonal Fluxes and Disturbance-Induced Losses. *Science* 302:1554.

42. Hutyra L, Wofsy SC, Saleska SR (2008) LBA-ECO CD-10 CO2 and H2O Eddy Fluxes at km 67 Tower Site, Tapajos National Forest. *Oak Ridge National Laboratory Distributed Active Archive Center*. Available at: http://www.daac.ornl.gov.

43. Miller SD, Goulden ML, Rocha HR (2009) LBA-ECO CD-04 Meteorological and Flux Data, km 83 Tower Site, Tapajos National Forest. *Oak Ridge National Laboratory Distributed Active Archive Center*. Available at: http://daac.ornl.gov.

44. Miller SD, Goulden ML, Rocha HR (2009) LBA-ECO CD-04 CO2 Profiles, km 83 Tower Site, Tapajos National Forest. *Oak Ridge National Laboratory Distributed Active Archive Center*. Available at: http://daac.ornl.gov.

45. Hutyra LR et al. (2008) Resolving systematic errors in estimates of net ecosystem exchange of CO2 and ecosystem respiration in a tropical forest biome. *Agricultural and Forest Meteorology* 148:1266–1279.

46. Bruno RD, Rocha H, Freitas H, Goulden ML, Miller SD (2008) LBA-ECO CD-04 Soil Moisture Data, km 83 Tower Site, Tapajos National Forest. *Oak Ridge National Laboratory Distributed Active Archive Center*. Available at: http://daac.ornl.gov.

47. Silver WL et al. (2005) Fine root dynamics and trace gas fluxes in two lowland tropical forest soils. *Global Change Biology* 11:290-306.

48. Palace M, Keller M, Asner GP, Silva J, Passos C (2007) Necromass in undisturbed and logged forests in the Brazilian Amazon. *Forest Ecology and Management* 238:309–318.

49. Telles EC et al. (2003) Influence of soil texture on carbon dynamics and storage potential in tropical forest soils of Amazonia. *Global Biogeochemical Cycles* 17:1040.

Figure Legends

Figure 1. Ground-based measurements of carbon accumulation in wood and soil water withdrawal at the logged site in Tapajos National Forest, Para, Brazil. a) Wood production versus tree height before (Nov 2000-Sep 2001, open squares) and after (Oct 2001-Mar 2004, solid circles) logging for 734 trees, normalized by total wood production. b) Water withdrawal versus depth at the logged site measured during the 2002 dry season (Aug-Nov) in an intact area (open squares) and within a logging gap (filled circles), normalized by total column water withdrawal for the same period. In both panels, the hatched (shaded) region corresponds to regions with increased (decreased) activity after logging.

Figure 2. Monthly forest-atmosphere fluxes of carbon (kg C $ha^{-1}d^{-1}$ and Mg C $ha^{-1}yr^{-1}$) and energy (W m^{-2}) at the control (km 67, dark curve) and logged (km 83, light curve) sites in Tapajos National Forest, Para, Brazil: a) GEE (positive to forest); b) respiration (positive to atmosphere); c) NEE (positive to atmosphere); d) sensible heat flux; and e) evaporation and precipitation (mm d^{-1}). Shaded areas about curves correspond to 95% percent confidence intervals due to sampling error, gap filling, and, for A,B, and C, the u_*-filter cutoff (0.17-0.27 m s^{-1}). Vertical shaded region Sep 15-Dec 15 2001 indicates logging period. Horizontal dashed lines indicate the logged-site average during period prior to logging.

Figure 3. Annual differences in forest-atmosphere carbon (Mg C $ha^{-1}yr^{-1}$) and energy (W m^{-2}) fluxes, calculated as (Δ=logged-unlogged), in Tapajos National Forest, Para, Brazil. The flux difference for the period prior to logging was subtracted from each post-logging period. a) GPP (positive to forest); b) respiration (positive to atmosphere); c) NEE (positive to atmosphere); d)

sensible heat flux; and e) latent heat flux. Vertical shaded region Sep 15-Dec 15 2001 indicates logging period. Error bars correspond to 95% percent confidence intervals due to sampling error and gap filling.

Figure 4. Carbon pools (boxes, Mg C ha^{-1}) and fluxes (arrows, Mg C ha^{-1}yr^{-1}): a) before logging; and b) for the 3-year period following logging (Table S4, Supplemental Information). Carbon pools include live plant biomass (186) (29), necromass (58.4) (48), and soil mineral carbon (71) (49).

Figure 1. Ground-based measurements of carbon accumulation in wood and soil water withdrawal at the logged site in Tapajos National Forest, Para, Brazil. a) Wood production versus tree height before (Nov 2000-Sep 2001, open squares) and after (Oct 2001-Mar 2004, solid circles) logging for 734 trees, normalized by total wood production. b) Water withdrawal versus depth at the logged site measured during the 2002 dry season (Aug-Nov) in an intact area (open squares) and within a logging gap (filled circles), normalized by total column water withdrawal for the same period. In both panels, the hatched (shaded) region corresponds to regions with increased (decreased) activity after logging.

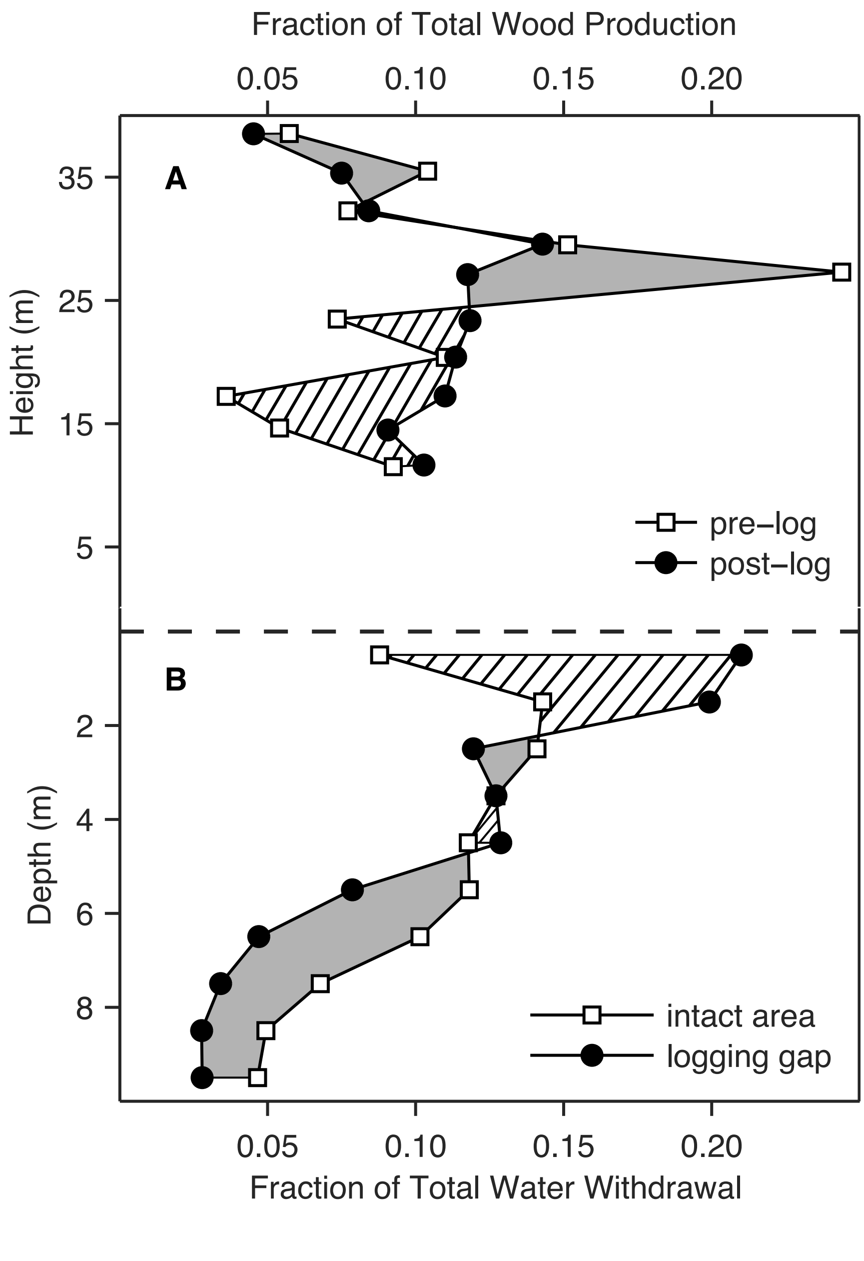

Figure 2. Monthly forest-atmosphere fluxes of carbon (kg C $ha^{-1}d^{-1}$ and Mg C $ha^{-1}yr^{-1}$) and energy (W m^{-2}) at the control (km 67, dark curve) and logged (km 83, light curve) sites in Tapajos National Forest, Para, Brazil: a) GEE (positive to forest); b) respiration (positive to atmosphere); c) NEE (positive to atmosphere); d) sensible heat flux; and e) evaporation and precipitation (mm d^{-1}). Shaded areas about curves correspond to 95% percent confidence intervals due to sampling error, gap filling, and, for A,B, and C, the u_*-filter cutoff (0.17-0.27 m s^{-1}). Vertical shaded region Sep 15-Dec 15 2001 indicates logging period. Horizontal dashed lines indicate the logged-site average during period prior to logging.

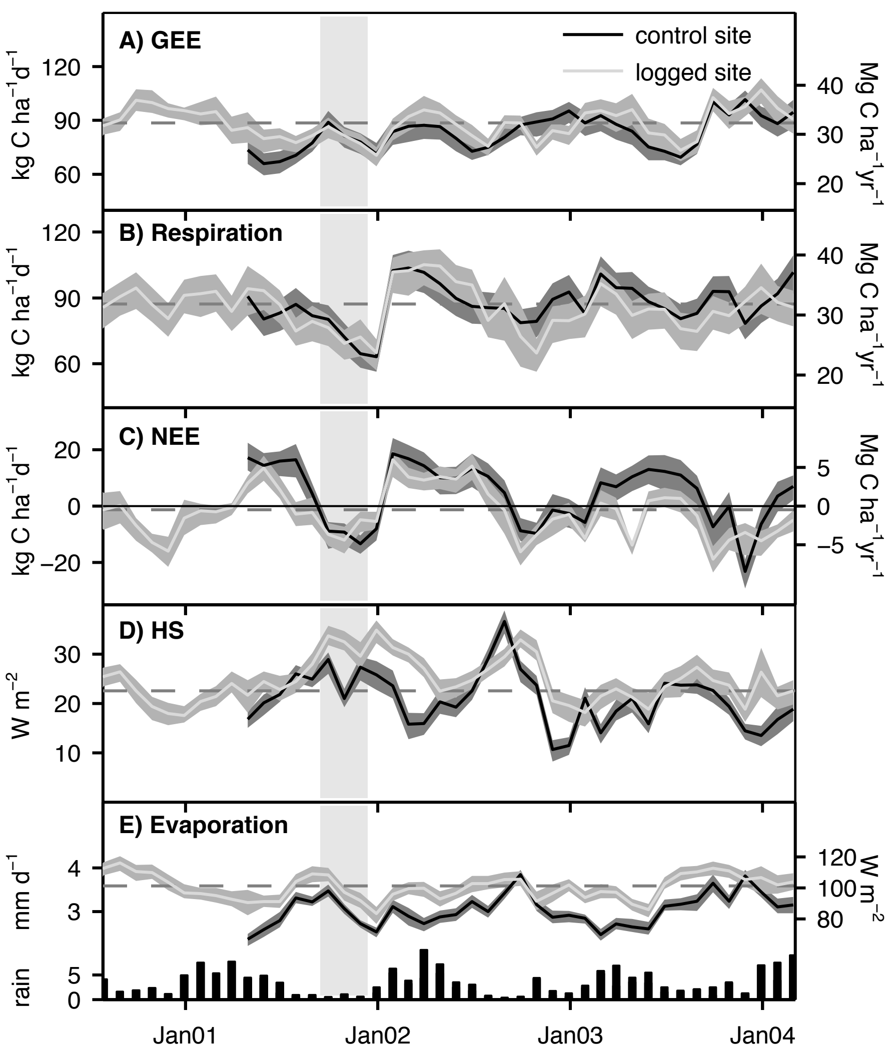

Figure 3. Annual differences in forest-atmosphere carbon (Mg C $ha^{-1}yr^{-1}$) and energy (W m^{-2}) fluxes, calculated as (Δ = logged-unlogged), in Tapajos National Forest, Para, Brazil. The flux difference for the period prior to logging was subtracted from each post-logging period. a) GPP (positive to forest); b) respiration (positive to atmosphere); c) NEE (positive to atmosphere); d) sensible heat flux; and e) latent heat flux. Vertical shaded region Sep 15-Dec 15 2001 indicates logging period. Error bars correspond to 95% percent confidence intervals due to sampling error and gap filling.

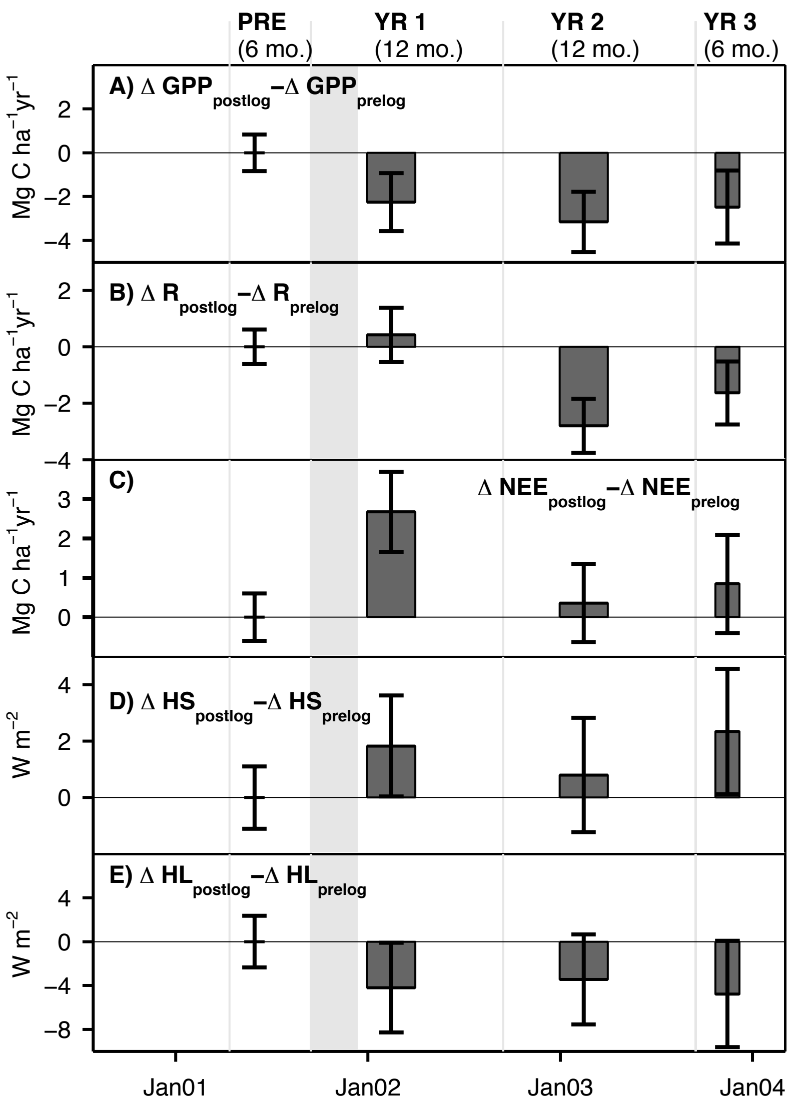

Figure 4. Carbon pools (boxes, Mg C ha^{-1}) and fluxes (arrows, Mg C ha^{-1}yr^{-1}): a) before logging; and b) for the 3-year period following logging (Table S4, Supplemental Information). Carbon pools include live plant biomass (186) (29), necromass (58.4) (48), and soil mineral carbon (71) (49).

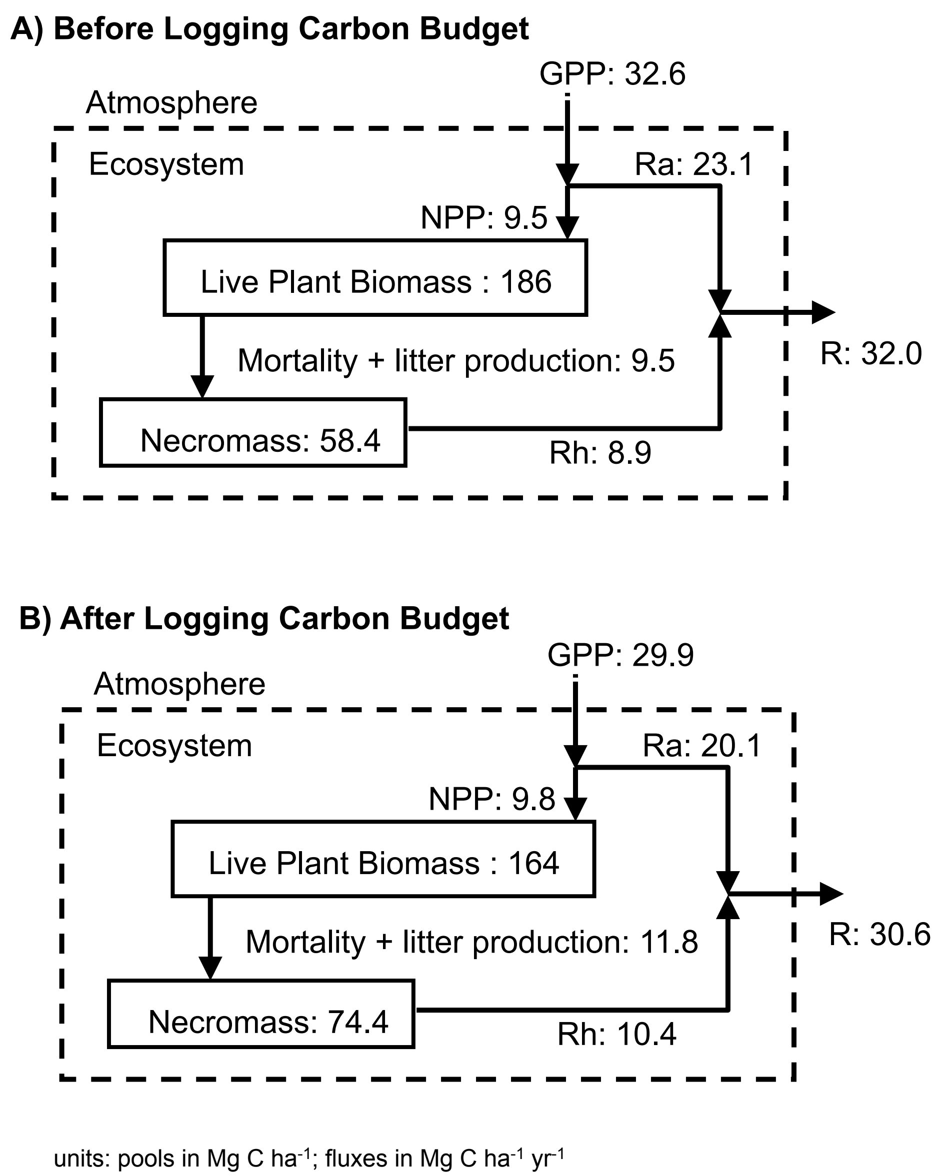

Supporting Information: Reduced Impact Logging Minimally Alters Tropical Rainforest Carbon and Energy Exchange

S1. Logging damage surveys

A post-logging survey in Dec 2001 of an 18-ha plot (600 m E-W x 300 m N-S) east of the eddy covariance tower found that 70 trees had been logged with an average diameter at breast height (DBH) of 82 cm. Bole wood from 65 of the trees had been removed from the site, while entire boles from the other 5 trees remained on the forest floor. The average length of bole moved off site was 20 m tree^{-1}, estimated as the distance between the stump and the remaining crown, corresponding to 5.9 ±0.9 Mg C ha^{-1}. The remaining bole wood (3.2 ±0.5 Mg C ha^{-1}) remained on the forest floor as coarse woody debris (CWD). The post-logging damage survey data are available online (1).

304 trees had damaged canopies, with the average canopy loss of 57%, while 447 trees had their bole snapped at an average height of 6.8 m. The biomass deposited to the forest floor from killed and damaged trees amounted to 5.8 ±1.0 Mg C ha^{-1}, while another 0.9 ±0.2 Mg C ha^{-1} of dead biomass remained standing (Table S1). Total CWD was 14.9 ±2.4 Mg C ha^{-1}. Logging-induced leaf and fine litter debris were estimated based on litter production rates measured at the logged site (2) and control site (3), assuming a 1-year turnover time. The leaf and fine litter data are available online (4, 5).

S2. Flux footprints

The logging extended roughly 3 km in the upwind (east) direction of the flux tower. Estimates of the flux footprint were calculated using an analytical model (6). During daytime, 80% of the flux was accumulated within 1 km of the tower, and >90% of the flux within 3 km. During nighttime, 60% of the flux was accumulated within the 3 km extent of the logging. We compared measured nighttime NEE when $u_* > 0.22$ m s^{-1} with an independent estimate of ecosystem respiration obtained from a light response model applied only to *daytime* measurements, when the flux footprint was within the extent of the logging. A comparison of these two independent estimates of R showed good agreement (7).

S3. Use of un-logged site as experimental control

Measurements at both the un-logged and logged sites suggested that their carbon pools and fluxes were not in steady state at the start of the experiment. The sites were found to have higher-than-expected proportions of small trees, (3, 8), and large amounts of coarse woody debris (CWD) on the forest floor (3, 9, 10). At the un-logged site, CWD decreased over a several year period (3). These observations were consistent with a pre-experiment disturbance at the Tapajos forest. This possibility was reinforced by observations of increased allocation of GPP to wood growth, and less to respiration, at the un-logged Tapajos site compared with forests in the central and eastern Amazon (11). The nature and timing of a pre-experiment disturbance has been hypothesized, yet remains unknown (12, 13). Alternatively, it has been suggested that the large CWD pools could be consistent with higher turnover rates in the Tapajos Forest relative to other Amazonian forests (14).

To examine the sensitivity of our results to a possible pre-logging disturbance at Tapajos, we calculated the inter-site NEE difference, ΔNEE, using different scenarios that represent end members for the possible impact of a pre-logging disturbance at Tapajos. The first assumption was that either there was no pre-logging disturbance at either Tapajos site, or that any disturbance affected the sites equally. In this scenario, the measured NEE at km 67 (Fig. S2a dark shaded boxes) was used to calculate the inter-site difference, ΔNEE (Fig. S2b dark shaded boxes). This case was used in Figure 3c.

The second scenario is that km 67 was disturbed prior to logging, while km 83 was not. For this scenario, an ecosystem carbon box model was developed to simulate the transient transfer of carbon among live and dead pools as the forest moved toward a steady state, using comprehensive measurements of carbon pools and fluxes from the un-logged site as model inputs (Fig. S2a, dashed curve) (12). The model indicated a net loss of carbon from the un-logged site that decreased slowly throughout the study interval. Adjusting the measured control site NEE to account for the modeled disturbance recovery showed a net carbon balance closer to zero (Fig. S2a, light boxes). The adjustment had a minor effect on ΔNEE when the post-logging changes were calculated relative to the pre-logging ΔNEE (Fig. S2b). Without the adjustment, ΔNEE for the first 3 years after logging was 1.4 relative to the pre-logging period, compared to 0.9 with the adjustment (Table S3). The difference between ΔNEE with and without adjustment was within the measurement uncertainty; therefore, the possible effects of pre-logging disturbance did not affect our conclusion that RIL had only minor carbon cycle impacts.

References Supporting Information

1. Sousa A et al. (2008) LBA-ECO CD-04 Post-logging Damage Survey, Logged Forest Site, km 83 Tower Site, Tapajos National Forest. *Oak Ridge National Laboratory Distributed Active Archive Center*. Available at: http://daac.ornl.gov.

2. Goulden ML et al. (2004) Diel and seasonal patterns of tropical forest CO2 exchange. *Ecological Applications* 14:42-54.

3. Rice AH et al. (2004) Carbon balance and vegetation dynamics in an old-growth Amazonian forest. *Ecological Applications* 14:55–71.

4. Figueira AM et al. (2008) LBA-ECO CD-04 Leaf Litter Data, Logged Forest Site, km 83 Tower Site, Tapajos National Forest. *Oak Ridge National Laboratory Distributed Active Archive Center*. Available at: http://daac.ornl.gov.

5. Rice AH et al. (2008) LBA-ECO CD-10 Ground-based Biometry Data at km 67 Tower Site, Tapajos National Forest. *Oak Ridge National Laboratory Distributed Active Archive Center*. Available at: http://www.daac.ornl.gov.

6. Hsieh CI, Katul G, Chi T (2000) An approximate analytical model for footprint estimation of scalar fluxes in thermally stratified atmospheric flows. *Advances in Water Resources* 23:765-772.

7. Hutyra LR et al. (2008) Resolving systematic errors in estimates of net ecosystem exchange of CO2 and ecosystem respiration in a tropical forest biome. *Agricultural and Forest Meteorology* 148:1266–1279.

8. Figueira AM et al. (2008) Effects of selective logging on tropical forest tree growth. *JGR-Biogeosciences.*

9. Palace M, Keller M, Asner GP, Silva J, Passos C (2007) Necromass in

undisturbed and logged forests in the Brazilian Amazon. *Forest Ecology and Management* 238:309–318.

10. Wofsy SC, Rice AH, Saleska SR, Pyle EH, Hutyra LR (2008) LBA-ECO CD-10 Coarse Woody Debris Data at km 67 Tower Site, Tapajos National Forest. *Oak Ridge National Laboratory Distributed Active Archive Center*. Available at: http://www.daac.ornl.gov.

11. Malhi Y et al., others (2009) Comprehensive assessment of carbon productivity, allocation and storage in three Amazonian forests. *Global Change Biology* 15:1255–1274.

12. Pyle EH et al., others (2008) Dynamics of carbon, biomass, and structure in two Amazonian forests. *Journal of Geophysical Research. G. Biogeosciences* 113.

13. Saleska SR et al. (2003) Carbon in Amazon Forests: Unexpected Seasonal Fluxes and Disturbance-Induced Losses. *Science* 302:1554.

14. Keller M, Palace M, Asner GP, Pereira R, Silva J (2004) Coarse woody debris in undisturbed and logged forests in the eastern Brazilian Amazon. *Global Change Biology* 10:784-795.

Figure Legends

Figure S1. LandSat image of Tapajos National Forest, Para, Brazil. The flux tower locations shown as black X: control site (km 67), logged site (km 83), and the agricultural site (km 77). The N-S road is the Santarem-Cuiaba highway (BR163).

Figure S2. A) Averaged NEE (Mg C $ha^{-1}yr^{-1}$) at the control site (km 67) in the Tapajos National Forest, Para, Brazil: measured NEE (dark box plots), modeled NEE due to disturbance (dashed curve) (Pyle et al. 2008), and measured NEE adjusted for disturbance (light box plots). Horizontal line at center of each box plot is mean gap-filled NEE, shaded box plot limits are mean NEE for $u_*=0.17\ ms^{-1}$ and $u_*=0.27\ ms^{-1}$ filters. B) Difference between NEE at the logged and un-logged sites. Vertical hatched region Sep 15-Dec 15 2001 indicates logging period. Error bars on boxes are the uncertainty due to gap filling and sampling.

Table Legends

Table S1. Effect of logging on above ground biomass pools in an 18-ha plot east of eddy flux tower at Tapajos National Forest, Para, Brazil.

Table S2. Average fluxes of carbon (Mg C $ha^{-1}yr^{-1}$) and sensible and latent heat (Wm^{-2}) at the control (km 67) and logged (km 83) sites in Tapajos National Forest, Para, Brazil. All fluxes include sampling and gap-filling uncertainty. Carbon fluxes (GPP, R, NEE) for each site also include additive uncertainty due to u_*-filter cutoff (see Materials and Methods). Uncertainty in inter-site carbon flux differences (ΔGPP, ΔR, ΔNEE) was calculated as the square root of the sum of squared sampling and gap filling uncertainties at each site, while the u_*-filter uncertainty was not included as both sites were found to require the same filter cutoff (12). Values in parenthesis were calculated assuming a pre-experiment disturbance at the control site that did not occur at the logged site, as described in section S3.

Table S3. Remote sensing (MODIS) albedo at the logged (km 83) and control (km 67) sites in the Tapajos National Forest, Para, Brazil, and for a nearby pasture site (km 77). Ratios of sites include only times when valid data available at both sites. The 95% confidence interval ranged 0.003-0.005, calculated using a bootstrap method.

Table S4. Carbon budget from ecological and meteorological measurements at the logged site at Tapajos National Forest, Brazil, for the year before and 3 years after Reduced Impact Logging (see Fig. 4). Positive GPP, NEP, NPP, and live biomass for carbon flux to forest; positive R, necromass, and decomposition for carbon flux from forest. Calculation of changes in the fluxes and their uncertainties described in Materials and Methods. All quantities in Mg C ha^{-1} yr^{-1}.

Table S5. Tree DBH increment rate (cm yr^{-1}) and wood production (Mg C $ha^{-1}yr^{-1}$) at the logged and control sites in the Tapajos National Forest, Para, Brazil, measured using dendrometer bands, for the 6-month period before logging, and 36-month period after logging.

Table S1. Effect of logging on above ground biomass pools in an 18-ha plot east of eddy flux tower at Tapajos National Forest, Para, Brazil.

	Per tree (Mg C)	Sum of trees (Mg C)	Density (Mg C ha^{-1})
Logged tree biomass[a]	3.2-4.4	224-306	12.5-17
Bole removed from site	1.3-1.7	89-122	5.0-6.8
Bole remaining (CWD)	0.7-0.9	48-65	2.7-3.6
Crown down (CWD)	1.3-1.8	90-123	5-6.9
Damaged/killed tree biomass	-	252-352	14-20
Damaged/killed CWD (forest floor)	-	86-120	4.8-6.7
Damaged/killed CWD (standing)	-	13-19	0.7-1.0
Total CWD added to forest floor	-	224-308	12.5-17.2

a. Biomass calculated as a range with the low end based on allometric equations for trees in Manaus, Brazil, and the high end for a range of tropical moist forests (14). Since biomass of sub-pools (boles, crowns) was only reported by Chambers et al. (2001) using the Manaus allometry, a factor 1.4 was used to calculate subpool biomass for the tropical moist forest allometry.

Table S2. Average fluxes of carbon (Mg C $ha^{-1}yr^{-1}$) and sensible and latent heat (Wm^{-2}) at the control (km 67) and logged (km 83) sites in Tapajos National Forest, Para, Brazil. All fluxes include sampling and gap-filling uncertainty. Carbon fluxes (GPP, R, NEE) for each site also include additive uncertainty due to u_*-filter cutoff (see Materials and Methods). Uncertainty in inter-site carbon flux differences (ΔGPP, ΔR, ΔNEE) was calculated as the square root of the sum of squared sampling and gap filling uncertainties at each site, while the u_*-filter uncertainty was not included as both sites were found to require the same filter cutoff (12). Values in parenthesis were calculated assuming a pre-experiment disturbance at the control site that did not occur at the logged site, as described in section S3.

	GPP (MgC $ha^{-1}yr^{-1}$)	R (MgC $ha^{-1}yr^{-1}$)	NEE (MgC $ha^{-1}yr^{-1}$)	H_S ($W m^{-2}$)	H_L ($W m^{-2}$)
Control Site (Km 67)					
Before logging (6 months)	26.0 ± 1.5	30.9 ± 2.5	4.9 ± 1.5 (2.2 ± 1.5)	21.5 ± 0.8	79.3 ± 1.6
Years 1-3 after	31.1 ± 1.4	32.1 ± 2.3	1.0 ± 1.2 (-1.0 ± 1.2)	20.4 ± 0.3	85.3 ± 0.6
Logged Site (Km 83)					
Before Logging (12 months)	32.6 ± 1.3	31.9 ± 1.7	-0.6 ± 0.8	22.5 ± 0.6	100.4 ± 1.2
Before Logging (6 months)	29.6 ± 1.8	31.2 ± 1.9	1.7 ± 0.9	25.1 ± 0.9	99.0 ± 1.7
Years 1-3 after	32.0 ± 1.1	31.0 ± 1.6	-1.0 ± 0.7	25.8 ± 0.4	101.3 ± 0.8
Logged Site-Control Site	ΔGPP	ΔR	ΔNEE	ΔH_S	ΔH_L
Before Logging (6 months)	3.6 ± 0.9	0.4 ± 0.6	-3.3 ± 0.6 (-0.6 ± 0.6)	3.6 ± 1.1	19.7 ± 2.4
Years 1-3 after	0.9 ± 0.3	-1.1 ± 0.2	-2.0 ± 0.3 (0.3 ± 0.3)	5.4 ± 0.4	15.7 ± 1.0

Table S3. Remote sensing (MODIS) albedo at the logged (km 83) and control (km 67) sites in the Tapajos National Forest, Para, Brazil, and for a nearby pasture site (km 77). Ratios of sites include only times when valid data available at both sites. The 95% confidence interval ranged 0.003-0.005, calculated using a bootstrap method.

	Year Before	Year 1-3 after
MODIS albedo		
km 67 (control site)	0.142	0.136
km 83 (logged site)	0.145	0.139
km 77 (pasture site)	0.154	0.168
Inter-site Ratios		
km 83/km67	1.03 ± 0.04	1.04 ± 0.02
km 77/km67	1.24 ± 0.04	1.34 ± 0.03

Table S4. Carbon budget from ecological and meteorological measurements at the logged site at Tapajos National Forest, Brazil, for the year before and 3 years after Reduced Impact Logging (see Fig. 4). Positive GPP, NEP, NPP, and live biomass for carbon flux to forest; positive R, necromass, and decomposition for carbon flux from forest. Calculation of changes in the fluxes and their uncertainties described in Materials and Methods. All quantities in Mg C ha^{-1} yr^{-1}.

	Before Logging	After logging	Change	Uncertainty in change
GPP	32.6	29.9	-2.7	2.5
R	32	30.5	-1.5	1.5
R_a=GPP-NPP	23.1	20.1	-3.0	3.5
R_h	8.9	10.4	1.5	2.7
NPP_{wood}	1.7	2.5	0.8	1.0
NPP_{leaf}	5.3	4.8	-0.5	1.6
NPP_{root}	2.5	2.5	0	1.0
NPP	9.5	9.8	0.3	2.2
Mortality	1.7	4.5	2.8	1.6
litter production	7.8	7.3	-0.5	1.9
Mortality+litter production	9.5	11.8	2.3	2.5
live biomass change	0	-2.0	-2.0	3.2
necromass change	0.6	1.4	0.8	3.7
NEP	0.6	-0.6	-1.2	1.3

Table S5. Tree DBH increment rate (cm yr^{-1}) and wood production (Mg C $ha^{-1}yr^{-1}$) at the logged and control sites in the Tapajos National Forest, Para, Brazil, measured using dendrometer bands, for the 6 month period before logging, and 36 month period after logging.

	Tree density ha^{-1}	# bands	Growth Rate (cm yr^{-1})		NPP_{wood} (Mg C $ha^{-1}yr^{-1}$)	
			Pre-log	Post-log	Pre-log	Post-log
Control Site	516	763[a]			3.1 ± 0.4	4.0 ± 0.5
10-35 cm	465	529	0.2 ±0.02	0.28 ± 0.03	1.7 ± 0.2	2.3 ± 0.2
35-55 cm	30	119	0.43 ± 0.05	0.52 ± 0.07	0.6 ± 0.1	0.7 ± 0.1
55-100 cm	21	115	0.41 ± 0.08	0.54 ± 0.09	0.7 ±0.2	1.0 ±0.2
Logged Site	482	691[b]			1.7 ± 0.4	3.4 ± 0. 4
10-35 cm	422	363	0.14 ±0.03	0.31 ± 0.03	0.9 ± 0.2	2.0 ± 0.2
35-55 cm	37	223	0.26 ± 0.05	0.47 ± 0.05	0.4 ±0.1	0.7 ± 0.1
55-100 cm	23	105	0.20 ± 0.08	0.43 ± 0.07	0.4 ± 0. 2	0.7 ± 0.1

a. Fewer bands than Rice et al. (2004) – we retained only bands that were in place as of Feb 2001, when logged site measurements began, and which were surveyed in 2001 and 2005.

b. More bands than the 234 reported Figueira et al. (2008). We retained additional bands by accounting for step changes in the data when the bands were readjusted.

Figure S1. LandSat image of Tapajos National Forest, Para, Brazil. The flux tower locations shown as black X: control site (km 67), logged site (km 83), and the agricultural site (km 77). The N-S road is the Santarem-Cuiaba highway (BR163).

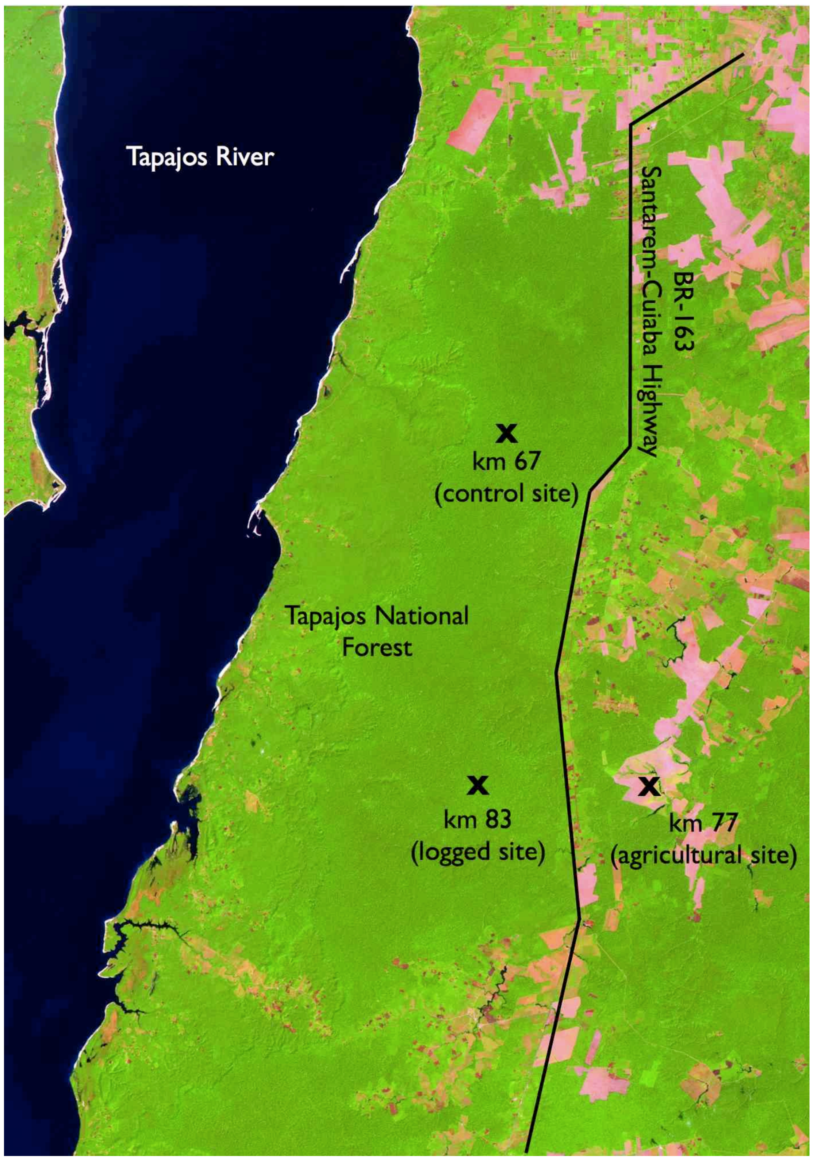

Figure S2. A) Averaged NEE (Mg C $ha^{-1}yr^{-1}$) at the control site (km 67) in the Tapajos National Forest, Para, Brazil: measured NEE (dark box plots), modeled NEE due to disturbance (dashed curve) (Pyle et al. 2008), and measured NEE adjusted for disturbance (light box plots). Horizontal line at center of each box plot is mean gap-filled NEE, shaded box plot limits are mean NEE for u_*=0.17 ms^{-1} and u_*=0.27 ms^{-1} filters. B) Difference between NEE at the logged and un-logged sites. Vertical hatched region Sep 15-Dec 15 2001 indicates logging period. Error bars on boxes are the uncertainty due to gap filling and sampling.